

AD-A073 657

CALIFORNIA UNIV BERKELEY ELECTRONICS RESEARCH LAB  
PLASMA THEORY AND SIMULATION.(U)  
MAR 79 C K BIRDSALL

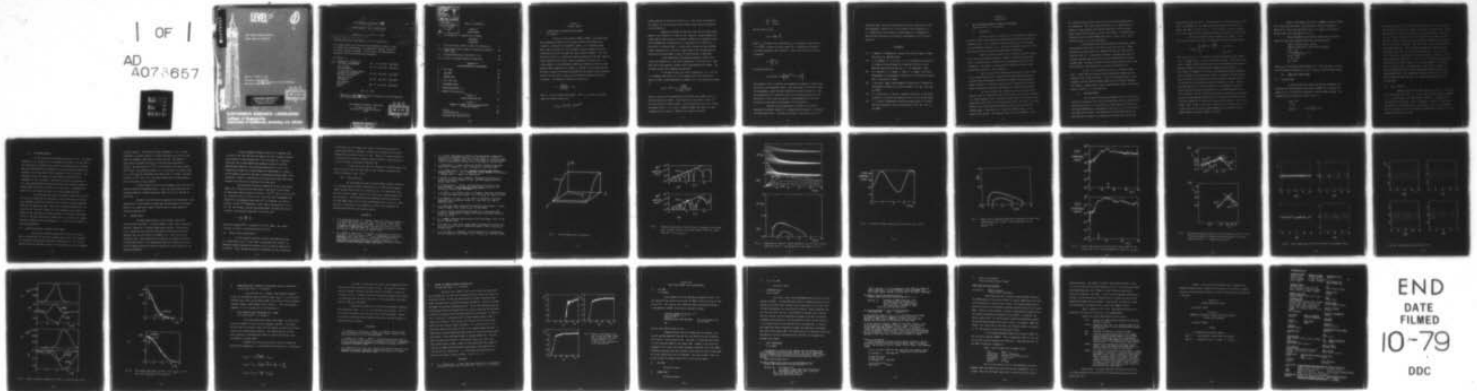
F/G 20/9

UNCLASSIFIED

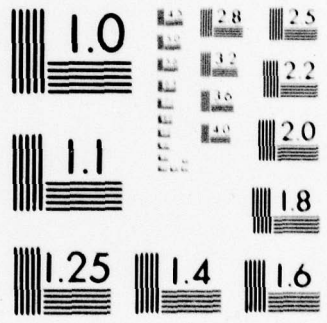
N00014-77-C-0579

NI

| OF |  
AD  
A073657



END  
DATE  
FILMED  
10-79  
DDC



MICROCOPY RESOLUTION TEST CHART  
NATIONAL BUREAU OF STANDARDS 1963-A

28

FIRST QUARTER PROGRESS REPORT ON  
PLASMA THEORY AND SIMULATION

January 1 - March 31, 1979

DOE Contract A503-76SF00034

(Project Agreement No. DE AT03-76ET53064)

ORR Contract N00014-78-C-0578

D D C  
RECEIVED  
SEP 11 1979  
REGISTRY  
D

80 07 16 061

**DISTRIBUTION STATEMENT A**

Approved for public release;  
Distribution Unlimited

9  
FIRST QUARTER PROGRESS REPORT, no. 1, 1 Jan -

6 PLASMA THEORY and SIMULATION, 31 Mar 79,

(January 1 to March 31, 1979)

15 N00014-77-C-0579  
Research during the first quarter of 1979 is reported here.

Our research group uses both theory and simulation as tools in order to increase the understanding of instabilities, heating, transport, and other phenomena in plasmas. We also work on the improvement of simulation, both theoretically and practically.

Our staff is —

10 Professor C. K. Birdsall (Principal Investigator)	191	M	Cory Hall	(642-4015)
Alex Friedman (Post Doctorate)	119	ME	Cory Hall	(642-3477)
Yu Jiuan Chen, Douglas Harned, Jae Koo Lee, Lee Buchanan (Research Assistants)	119	MD	Cory Hall	(642-1297)
Stephen Au-Yeung (Programmer)	119	MD	Cory Hall	(642-1297)
Mike Hoagland Research Typist	199	M	Cory Hall	(642-7919)

March 31, 1979

DOE Contract AS03-76SE00034 (Project Agreement No. DE AT03-76ET53064)  
ONR Contract N00014-77-C-0578

ELECTRONICS RESEARCH LABORATORY  
College of Engineering  
University of California, Berkeley  
94720

DDC  
RECEIVED  
SEP 11 1979  
REGULATED  
D

(i)

DISTRIBUTION STATEMENT A  
Approved for public release;  
Distribution Unlimited

127 550 mt

Accession For	
NTIS GRA&I	<input checked="" type="checkbox"/>
DDC TAB	<input type="checkbox"/>
Unannounced	<input type="checkbox"/>
Justification	<input type="checkbox"/>
By <i>Per Hr. on file</i>	
Distribution/	
Availability Codes	
Dist.	Avail and/or special
<b>A</b>	

TABLE of CONTENTS;

*Section I*

PLASMA THEORY

- A. → Filamentation in Charged Particle Beams; 1

*SECTION II*

SIMULATION

- A. Drift-Cyclotron Instability Particle Simulations; 5
- B.\* → Lower Hybrid Drift Instability Simulations Using ES1 Hybrid Code; 26
- C.\* → Field Reversed Layer Simulations in 1d; 26
- D.\* → Control of Unwanted Beaming Instabilities; 28

*Section III*

CODE DEVELOPMENT and MAINTENANCE

- A. → ES1 Code; 30
- B. EM1 Code 30
- C. EZOHAR Code 30
- D. ES1 + EFL Code 31
- E. → RINGHYBRID Code; 31
- F. → RJET Development; and 31
- G. → DDEX Utility Routine; 33

*Section IV*

PLASMA SIMULATION TEXT

35

*Section V*

SUMMARY of REPORTS, TALKS and PUBLICATIONS  
in THE PAST QUARTER

35

- Errata 35
- Distribution List 36

\* Indicates ONR supported areas

*Section 1*  
PLASMA THEORY

A. FILAMENTATION IN CHARGED PARTICLE BEAMS

Lee Buchanan

Since the classic paper of Weibel (1959), it has been known that homogeneous plasmas with anisotropic velocity distributions are unstable to transverse electromagnetic modes. In a streaming plasma, these modes, also known as "tearing modes", manifest themselves as the transverse pinching of the beam into small current filaments. This filamentation results in a significant transverse heating of the beam, inducing radial expansion which grossly affects propagation, focusing, etc. A simple example is given by Benford (1973) who considers an infinite, homogeneous beam streaming with a velocity  $v_0$  through a collisionless plasma. The beam is taken to be charge neutralized by the plasma and the transverse velocity distribution is taken to be Lorentzian (allowing closed form solutions). The dispersion relation is found to be

$$i\omega = \frac{\omega_B k_{\perp} v_0}{\sqrt{\omega_p^2 + k_{\perp}^2 c^2}} - k_{\perp} v_{\perp}$$

where  $k$  is the transverse wave number. When  $v_{\perp} < v_0$  there are unstable modes with maximum growth rate

$$(i\omega)_{\max} = \frac{\omega_p}{c} \left( v_0^{2/3} - v_{\perp}^{2/3} \right)^{3/2}$$

clearly showing the stabilizing effect of  $v_0$ . This can be interpreted as the tendency for an anisotropic beam to seek isotropy using the mechanism of the instability.

Exhaustive treatment of both the linear and non-linear development of the instability is found in the literature. Rather complete non-linear analytic descriptions of the Weibel instability are compared to one- and two-dimensional simulations by R. C. Davidson et al. (1972) and R. L. Morse and C. W. Nielson (1971). Of particular interest are the two-dimensional simulations of R. Lee and M. Lampe (1973) of the filamentation of relativistic electron beams in which the microstructure is described.

In the regime where the background plasma is highly collisional and conductivity is low, the filamentation is non-resistive in character and is more generally termed fluting (interchange) and firehose. The two have received quite adequate consideration.

In the case of high, but finite, conductivity, E. P. Lee and F. W. Chambers have found, for a fully charge and current neutralized beam in a highly ionized background of conductivity  $\sigma$ , the dispersion relation is

$$4\pi\rho i\omega = c^2 k^2 + \frac{v_0^2 k_{\perp}^2 \omega_B^2}{(\omega - v_B k_{\parallel} + i k_{\perp} \Delta v)^2}$$

where  $k_{\perp}$  and  $k_{\parallel}$  are the perpendicular and parallel wave numbers and  $v_0$  is the beam velocity as before. Substitution of  $\rho = en\mu$  where  $\mu = e/m(v - i\omega)$  and letting the collision frequency  $\nu$  and the parallel  $k$  go to zero recovers the Benford result. For finite  $\rho$ , Chambers (1978) finds that for a self-pinched beam (e.g. Bennett, 1939) one can invoke the relation

$$\frac{\Delta v^2}{v_0^2} \approx \frac{I_{\text{net}}}{I_{\text{Alfven}}}$$

and the condition that

$$I_{\text{net}} = I_{\text{BEAM}} \frac{\tau_p}{\tau_m}$$

where  $\tau_p$  is the beam pulse duration and  $\tau_m$  is the magnetic decay time ( $\tau_m = 4\pi\rho/c^2 k_{\perp}^2$ ), to obtain the total growth for a transverse perturbation to a beam streaming in the z-direction. This can be written in terms of a parameter

$$\Lambda = \frac{z^2 c^2}{\omega_B^2} \frac{\tau_p}{\tau_m}$$

so that one obtains as

$$\text{total growth} \approx \exp \left[ \left( \frac{27}{4} \right)^{1/3} \Lambda^{1/3} - \frac{1}{2} \Lambda^{1/2} \right].$$

This analytic result is based on the assumption of constant, isotropic conductivity of the background plasma. Since the growth is a sensitive competition between a growth term and a damping term, both functions of  $\rho$ , one may conclude that the transverse structure of  $\rho$  and particularly the time evolution of  $\rho$  due to the ionization of the background by the beam may be crucial to the onset and development of the instability.

Presently we are undertaking to simulate in one and two dimensions the Weibel instability in charged particle beams in a background of finite conductivity. We intend to construct a particle/fluid hybrid

simulation code in which the beam consists of finite sized particles and the background is taken to be a fluid plasma of finite conductivity  $\sigma$ . It is expected that the new physics should appear as a consequence of both the self-consistent time and spatial development of the fluid conductivity.

#### REFERENCES

- (1) G. Benford, "Filamentation in Relativistic Electron Beams", *Plasma Physics* 15, pp. 483-499 (1973).
- (2) F. W. Chambers, E. P. Lee, and S. S. Yu, "Filamentation Instability of a Heavy Ion Beam Propagating Through Gas", *Bulletin of the American Physical Society* 23, No. 7, p. 770 (September, 1978).
- (3) R. C. Davidson, D. A. Hammer, I. Haber, C. E. Wagner, "Non-linear Development of Electromagnetic Instabilities in Anisotropic Plasmas", *Phys. Fluids* 15, 317 (1972).
- (4) R. Lee and M. Lampe, "Electromagnetic Instabilities, Filamentation, and Focusing of Relativistic Electron Beams", *Phys. Rev. Lett.* 31, 23 (1973).
- (5) R. L. Morse and C. W. Nielson, "Numerical Simulation of the Weibel Instability in One and Two Dimensions", *Phys. Fluids* 14, 830 (1971).
- (6) E. S. Weibel, "Spontaneously Growing Transverse Waves in a Plasma due to an Anisotropic Velocity Distribution", *Phys. Rev. Lett.* 2, 83 (1959).

## SECTION II SIMULATION

### A. DRIFT-CYCLOTRON INSTABILITY PARTICLE SIMULATIONS

Jae Koo Lee (Prof. C. K. Birdsall)

#### I. INTRODUCTION

The drift-cyclotron instability is a collisionless instability occurring in any finite plasma with a Maxwellian velocity distribution in a magnetic field. This instability might constitute a part of the major plasma confinement problems in e.g., most mirror machines like 2XII $\beta$  or TMX even after the drift-cyclotron-loss-cone mode is stabilized.

Recent theoretical studies [1] of the drift-cyclotron instability have attracted much attention; however, they have had some difficulty in providing useful information on the nonlinear evolution of this instability. Our object is to use particle simulation to obtain linear and nonlinear behavior of this instability.

One recent particle simulation of the drift-cyclotron instability is one-dimensional [2], treating the electron effects as those of a linear fluid and assuming a fixed density gradient, thus reducing the spatial dimension in simulation from two to one. These results provide useful information but have the shortcoming of a fixed density gradient.

We have simulated this instability using a two-dimensional particle code for a Maxwellian velocity distribution with a density gradient in a uniform magnetic field. During the linear stage, our simulations show exponential growth over a few ion cyclotron periods. We compare this linear behavior with linear theory which does not use the local approximation because  $a_i/R_p$  is large (here,  $a_i$  is the ion gyroradius and  $R_p$  is the density scale length). This nonlocal theory is that of ROOTS [3], which

has a periodic guiding center density profile unlike the bounded one in our simulations. The linear growth rates and (in less degree) the frequencies in the simulations are found to agree well with the nonlocal theory predictions (and poorly with the local theory). The comparison of simulation with the nonlocal ROOTS predictions is given in Sec. III for two mass ratios, i.e.,  $m_i/m_e = 100$  and 25.

At saturation, the total electrostatic field energy reaches a few percent of the initial ion kinetic energy for most runs. These simulation saturation levels are compared with some existing nonlinear theories in Sec. IV. At and after saturation, the phase space plots of electrons and ions show vortex-like structure corresponding to the most unstable mode; the density profiles of each species become flatter as has been observed in lower-hybrid-drift instability simulations [4].

In Sec. II, a brief description of our simulation model is given. Growth rates and frequencies are compared with theoretical predictions in Sec. III for two cases. In Sec. IV, nonlinear aspects of this instability are discussed including comparison with nonlinear frequency shift theory, trapping theory, density-gradient modification, and electron heating. Section V is the conclusion.

## II. SIMULATION MODEL

For our study of the density-gradient-driven drift-cyclotron instability, we need to use a fully two-dimensional particle code for both electrons and ions, i.e., the evolution of four phase space variables in the plane perpendicular to the magnetic field  $(x, y, v_x, v_y)$  of all the particles needs to be followed. The common guiding center approximation for electrons was not used in our simulations; electrons and ions are both

magnetized and fully nonlinear. The code we use is a two-dimensional electrostatic one, EZOHAR [5]. The coordinates and the density profile of the plasma slab model are shown in Fig. 1. For simplicity, all the simulation runs in this paper have no temperature gradient and initially cold electrons.

The initial particle spatial loading is as follows: first, the ion guiding center positions are determined from the following profile,

$$n_i(x_{gc}) = \begin{cases} n_0 \left( 1 + \cos \kappa \frac{x_{gc}}{a_i} \right) & x_{gc} < \pi a_i / \kappa \\ 0 & x_{gc} \geq \pi a_i / \kappa \end{cases} .$$

Here,  $x_{gc} = x + v_y / \omega_{ci}$ ,  $\kappa$  is a constant indicating the density scale length (i.e.,  $\kappa = a_i / R_p$ ), and  $\omega_{ci}$  is the ion cyclotron frequency. Then the ion gyroradius is added to these guiding center positions to determine the actual ion positions (velocities are chosen from a Maxwellian distribution). If this process is repeated for electrons, then appreciable charge separation results, because the guiding center profile is different from the particle density profile for the species with large gyroradius; these two profiles are the same for cold electrons as noted in Naitou et al. [6]. Instead, the actual positions of ions are copied in our simulations to give the actual electron positions, thus resulting in no charge separation at the initial loading. [As the instability developed, we sometimes observed charge separation producing appreciable electric field along the density gradient direction responsible for some collisionless plasma transport. This is discussed in Sec. IV (3).] The velocity loading is by "ring and spokes" in  $v_x$ - $v_y$  space with the ring radius chosen randomly to fit a Gaussian and the spokes (angles) are chosen randomly, uniformly.

Along  $x$ , the boundary conditions in EZOHAR are those of Naitou et al. [6] at the low density side and those of inversion symmetry of Nevins et al. [7] at the high density end,  $x=0$ . Along  $y$ , the system is periodic due to the slab model (cf. Fig. 1).

Typical parameters are as follows (these are to be varied widely but used unless otherwise specified in later Sections)

$$\text{number of spatial grids} = 32 \times 32$$

$$\text{number of electrons or ions} = 16 \times 16 \times 32 = 8192$$

$$\omega_{pe} \Delta t \sim 0.5$$

$$\kappa \equiv (a_i dn/dx/n)_{x=\frac{1}{2}L_x} \sim 0.5$$

$$m_i/m_e = 25-300$$

$$L_x = L_y = 8a_i$$

$$\lambda_{Di} \sim 0.2a_i$$

where  $\omega_{pe}$  is the electron plasma frequency,  $\Delta t$  is the time step,  $L_x$  and  $L_y$  are the simulation dimensions in  $x$  and  $y$ , and  $\lambda_{Di}$  is the ion Debye length.

### III. CHECK WITH LINEAR THEORY

#### (1) $m_i/m_e=25$ Case

In order to check the growth rates and the frequencies predicted by the linear nonlocal theory given by ROOTS [3], we made an all-mode run (i.e., no artificial truncation of Fourier modes was used). The parameters are (in addition to those in Sec. II)

$$m_i/m_e = 25$$

$$\kappa = 0.5$$

$$\omega_{pe}/\omega_{ce} = 1 \quad , \quad \text{thus } \omega_{pi}^2/\omega_{ci}^2 = 25 \quad .$$

The squared potentials for modes 5 and 9 are shown in Fig. 2A and 2B, which tend to follow the theoretical growth rates drawn as straight lines. Reasonable agreement in growth rates extends to most growing modes in the range,  $1.2 < ka_i < 3.6$  as summarized in Fig. 3B, which does not include the finite grid ( $\Delta x$ ) effect. We observed less satisfactory agreement in the measurement of oscillation frequencies. The solid lines in Fig. 3A show the non-local ROOTS theory [3]. The simulation frequencies are measured during approximately the first two ion cyclotron periods (i.e.,  $0 < \omega_{ci} t < 12$  as in Fig. 3) which is considered to be the linear stage. Figure 4 is a frequency spectrum for mode 3 (i.e.,  $ka_i = 1.2$  in Fig. 3) showing a quite broad spectrum with the width of about  $\frac{1}{2}$ -1 of the peak frequency. This broad width is due to the short time span used in fast Fourier transform; it could be reduced by having a longer linear growth period with just the growing mode excited. The frequencies of modes 7 and 8 in Fig. 3A also had a broad width around the peak  $\omega = 0$ , indicating the possibility of a vortex mode.

(2)  $m_i/m_e = 100$  Case

Another check with the linear theory was sought in a simulation run, where larger mass ratio (i.e.,  $m_i/m_e = 100$ ) and larger density gradient (i.e.,  $\kappa = 0.7$ ) were used in a lower density plasma (i.e.,  $\omega_{pe}^2/\omega_{ce}^2 = 0.15$ ). The growth rates are shown in Fig. 5; agreement is again fairly good considering that all the growing modes in this range,  $1 \leq ka_i \leq 6$ , were allowed to grow in a single run. The real frequencies produced broad spectra as in the previous small mass ratio case.

#### IV. NONLINEAR BEHAVIOR

For the study of the nonlinear evolution of the drift-cyclotron instability, our simulation uses single-mode runs; namely, only one mode in the y-direction is allowed to vary while the perturbed quantities (charge densities and potentials) corresponding to all the other mode numbers are truncated at all times after Fourier transform in the y-direction. This truncation includes the mode  $k_y = 0$  which implies charge neutrality; independent of this truncation, simulations start exactly charge-neutral. This single-mode assumption has been also used in the nonlinear theory of a beam-plasma instability by O'Neil et al. [8], and is a reasonable one especially in an instability study with a discrete mode spectrum.

Since exact particle movers are used for electrons as well as for ions, our simulations are restricted to using small mass ratios (e.g.,  $m_i/m_e = 25-300$ ) to keep the simulation errors and cost low when reasonably large time increments are used. This error or numerical heating was 1-2% of the initial ion kinetic energy up to the saturation time  $t$ , which is defined as the time when field energy reaches its first peak after growth. In Fig. 6, the total electrostatic energy, ESE, in a typical run is shown providing a growth of one to two decades (i.e., a factor of 10 to 100) in a few cyclotron periods.

##### (1) Check With Nonlinear Frequency Shift Theory

One possible saturation mechanism for the drift-cyclotron mode is the nonlinear ion cyclotron frequency shift [2,9], which proposes the scaling of the saturated electrostatic potential as  $\zeta \propto \kappa \delta^{1/2}$ . We conducted a series of parameter studies with single-mode runs (as in the above

nonlinear theory). The theoretical power dependence,  $\zeta \propto \delta^{\frac{1}{2}}$  is roughly recovered in a certain range of  $\delta$  in these simulation runs (see Fig. 7A), where all parameters other than  $\delta$  are kept the same. The change in  $\delta$  comes either from mass ratio  $m_i/m_e$  or from relative plasma density  $\omega_{ci}^2/\omega_{pi}^2$ . The new scaling  $\zeta \propto \delta^{-1}$  for  $\delta > 0.07$  (see Fig. 7A) has no theoretical origin. The predicted scaling,  $\zeta \propto \kappa$ , is verified in a certain range of  $\kappa$  in Fig. 7B, with simulation runs in which only  $\kappa$  is varied. The other scaling,  $\zeta \propto \kappa^{-3/4}$ , for  $\kappa > 0.7$ , has close relation with a trapping theory and is discussed in a later Section.

In these simulation runs for the parameter study, the real frequencies could not be measured clearly; thus, the classification of the simulation mode as to whether marginally stable or not as in [9] was not quite clear.

Related to this difficulty of measuring real frequencies is the generation of a zero-frequency (vortex) mode excited possibly by nonlinear effects or by quasilinear spatial diffusion due to charge separation studied by Sperling [10].

## (2) Trapping Theory

The phase space pictures in Fig. 8 reveal vortex-like structure after saturation. Since only mode 3 is kept, three vortices are seen here (especially in electron phase space pictures). Also observed in our simulations are relatively large electric potentials, which are necessary (but not sufficient) for trapping, i.e.,  $\zeta \sim 0.3 - 0.5$  at the saturation time. (These potentials are likely to be reduced with the use of larger mass ratios.) This observation leads us to examining the possibility of having the familiar particle (electrons or ions) trapping as the saturation mechanism.

We have attempted to measure the fall (or trapping) time,  $\tau_f$ , which is the time from the first peak to the first minimum of electrostatic potential, and the potential at its first peak,  $\phi_s$ , in various simulation runs to check whether the parameter scales as  $\tau_f \propto \phi_s^{-1/2}$  as expected when trapping is the saturation mechanism as in [11]. This attempt has not been very fruitful because the measurement of  $\tau_f$  and  $\phi_s$  carried somewhat large error bars due to complicated patterns shown in the simulations; however, a qualitative verification of the above scaling was recovered from some of our simulations (not shown here).

The discussion of electron trapping for a drift-cone mode by Aamodt [12] is found to be also applicable to the drift-cyclotron mode. His approximate model provides the scaling,  $\zeta \propto \delta^{1/2} \kappa^{-3/4}$ , which is his Eq. (6). Our simulation runs for  $\delta \leq 0.07$  in Fig. 7A verifies the  $\delta^{1/2}$  dependence (although this weak dependence could also be  $\delta^{1/2}$  as discussed in an earlier Section), and the  $\kappa^{-3/4}$  dependence is more clearly recovered for  $\kappa > 0.7$  in Fig. 7B. Even without using any approximate model (including the ion distribution), the saturation amplitude is by his Eq. (4),

$$\zeta = \frac{\omega}{\omega_{ci}} \frac{0.5}{ka_i} \frac{\Delta}{a_i}$$

where  $\phi(x) = \phi_0 \exp(-x^2/\Delta^2)$  is assumed as in his Eq. (A5A). This radial structure is similar to simulation results (Fig. 9).

### (3) Density Profile Modification

As the instability develops into the large amplitude stage, it is observed as in Fig. 10 that there is appreciable collisionless (or anomalous) plasma transport from the high to the low density region due to  $E \times B$  drifts. Thus, the density profiles (integrated over the y-direction)

of electrons and ions change their shapes, flattening macroscopically toward reduced density gradients, which may be considered the saturation mechanism as discussed in Lee et al. [13]. Again, this charge separation in the direction of density gradient might be related to the generation of the collisionless vortex mode of Sperling [10].

In contrast to Fig. 10A, Fig. 10B shows less modification of the density profile since this case seems to have different saturation mechanism as discussed in Sec. IV (a).

#### (4) Electron Heating

As the instability grows, electrons behave somewhat coherently with the wave especially before saturation (cf, Fig. 8A) and then develop thermal spreads near or after the saturation time. Our examination shows that this electron thermal spread is not sufficient to cause saturation of the instability. The threshold electron temperature predicted either by the local ROOTS theory [3] or by Gary and Sanderson [14] is  $T_e/T_i = 6$ , while the ratio at saturation in our simulation is 0.07, thus eliminating the saturation possibility by the electron heating.

#### REFERENCES

1. A. B. Mikhailovskii and A. V. Timofeev, "Theory of Cyclotron Instability in a Non-Uniform Plasma", Zh. Eksp. Teor. Fiz. 44, pp. 919-921 (1963) [Sov. Phys. JETP 17, pp. 626-627 (1963)]; N. A. Krall, "Drift Waves", in Advances in Plasma Physics (John Wiley and Sons, 1971), Vol. 1, pp. 153-199; A. K. Nekrasv, "Nonlinear Evolution of Drift-Cyclotron Flute Oscillations", Nucl. Fusion 14, pp. 865-872 (1974).
2. B. I. Cohen, N. Maron, and T. D. Rognlien, "A Local Theory of Nonlinear Ion Dynamics in a Drift-Cyclotron Mode", in Proceedings of Fusion Theory Conference (1978), Paper OA-5; B. I. Cohen and G. R. Smith, "Efficient Method for Local Simulation of Drift-Wave Instabilities", in Proceedings of the Eighth Conference on Numerical Simulation of Plasmas (Lawrence Livermore Laboratory, 1978), Paper PD-8.

3. M. J. Gerver, Memorandum No. M77/27, Electronics Research Laboratory, University of California, Berkeley, Oct. 31 (1976); M. J. Gerver, C. K. Birdsall, A. B. Langdon, and D. Fuss, "Normal Modes of a Loss Cone Plasma Slab with Steep Density Gradient", *Phys. Fluids* 20, pp. 291-300 (1977).
4. D. Winske and P. C. Liewer, "Particle Simulation Studies of the Lower Hybrid Drift Instability", *Phys. Fluids* 21, pp. 1017-1025 (1978).
5. A. B. Langdon and B. F. Lasinski, Methods in Computational Physics, (Academic Press, N. Y., N. Y., 1976), Vol. 16, pp. 327-361; W. M. Nevins, Y. Matsuda, and M. J. Gerver (in preparation).
6. H. Naitou, S. Tokuda, and T. Kamimura, "On Boundary Conditions for a Simulation Plasma in a Magnetic Field", IPPJ-307, Nagoya University, Nagoya, Japan (1977).
7. W. M. Nevins and M. J. Gerver, "Two Dimensional Electrostatic Code, Modified ZOHAR", in Second Quarter Progress Report, University of California, Berkeley, pp. 2-8 (1976).
8. T. M. O'Neil, J. M. Winfrey, and J. H. Malmberg, "Nonlinear Interaction of a Small Cold Beam and a Plasma", *Phys. Fluids* 14, pp. 1204-1212 (1971).
9. R. E. Aamodt, Y. C. Lee, C. S. Liu, and M. N. Rosenbluth, "Nonlinear Dynamics of Drift-Cyclotron Instability", *Phys. Rev. Lett.* 39, pp. 1660-1664 (1977).
10. J. L. Sperling, "Quasi-Linear Diffusion and Particle Transport in Inhomogeneous Plasmas", *Phys. Fluids* 21, pp. 221-223 (1978).
11. S. Seiler, "Linear and Nonlinear Development of a Lower-Hybrid Wave Driven by a Perpendicular Ion Beam", Ph.D. Thesis, Princeton University (1977), pp. 27-29.
12. R. E. Aamodt, "Electron Stabilization of Drift-Cone Modes", *Phys. Fluids* 20, pp. 960-962 (1977).
13. W. W. Lee, Y. Y. Kuo, and H. Okuda, "Numerical Simulations of Collisionless Drift Instabilities for Low-Density Plasmas", *Phys. Fluids* 21, pp. 617-626 (1978).
14. S. P. Gary and J. J. Sanderson, "Density Gradient Drift Instabilities: Oblique Propagation at Zero Beta", *Phys. Fluids* 21, pp. 1181-1187 (1978).

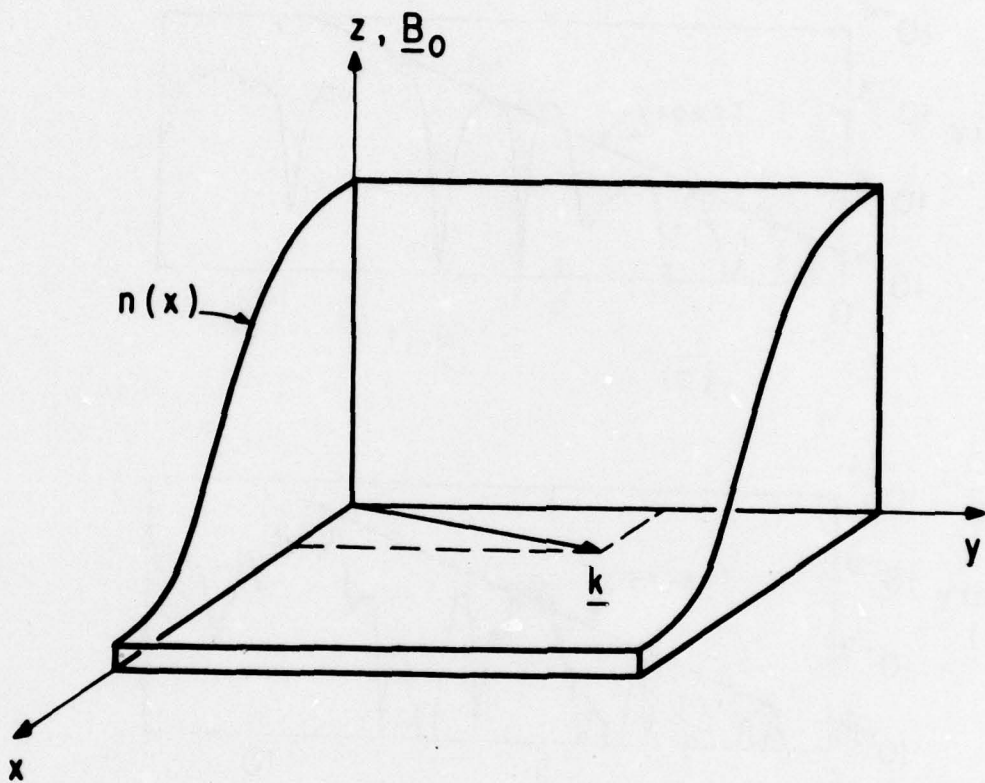


FIG. 1 The slab shape used in simulation.

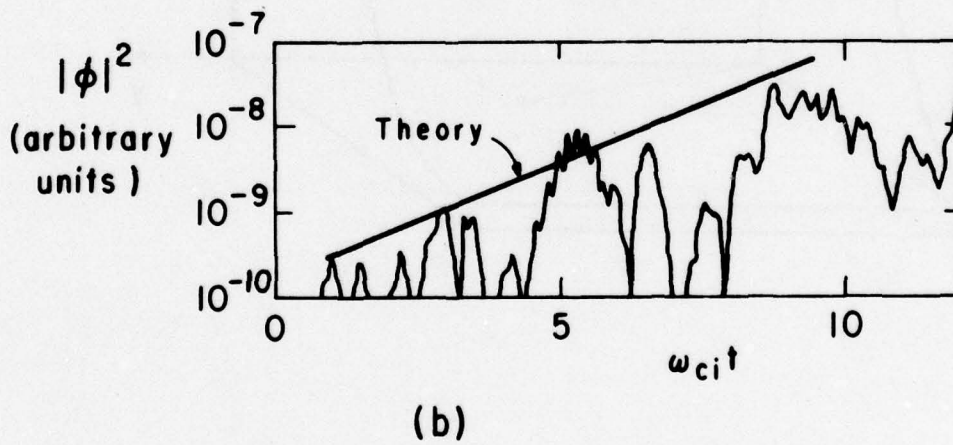
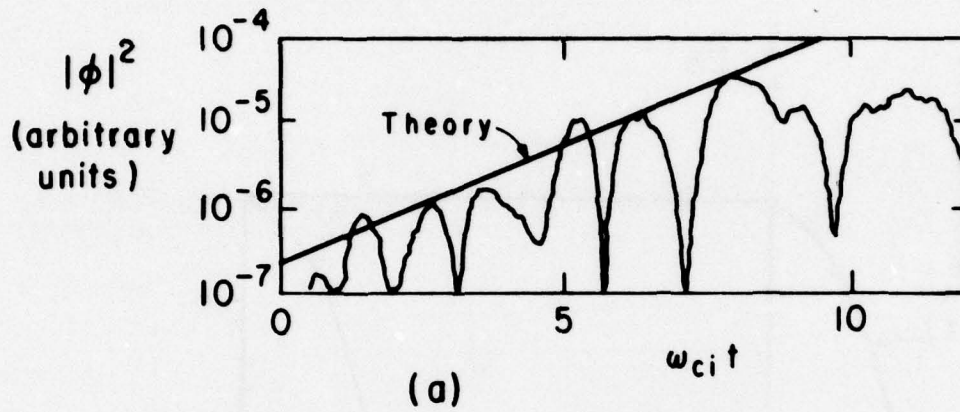


FIG. 2 Simulation electrostatic energy (curves) as compared to the growth rates (straight lines) of the linear nonlocal theory [3]. Here  $m_i/m_e = 25$ ,  $\kappa = 0.5$ ,  $\omega_{pe}/\omega_{ce} = 1$ .

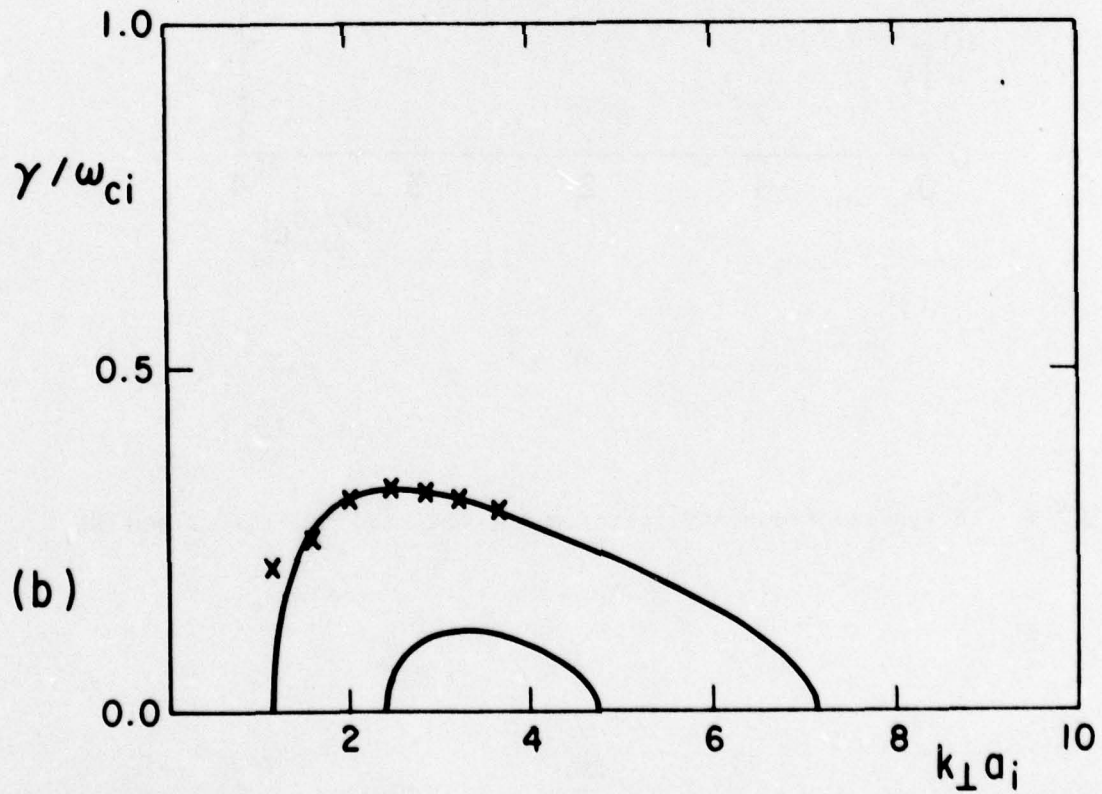
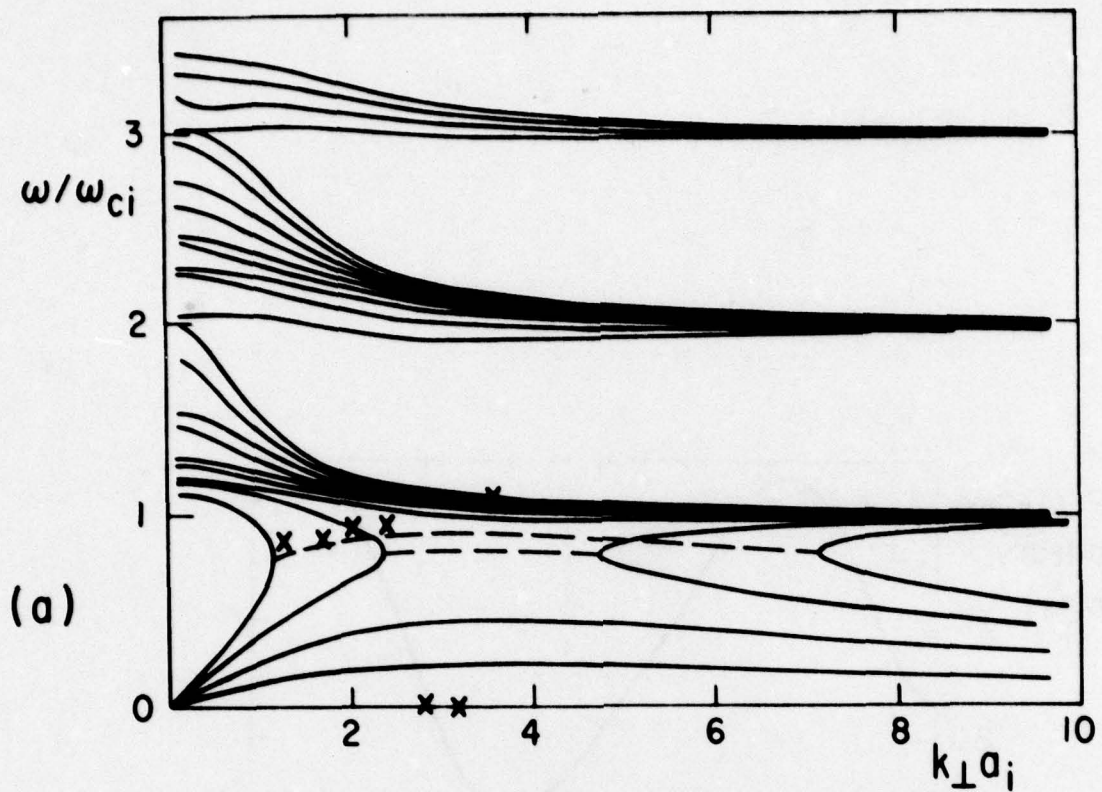


FIG. 3 Comparison of simulation results (marked X) with the linear nonlocal theory [3] (curves). The parameters are the same as in Fig. 2.

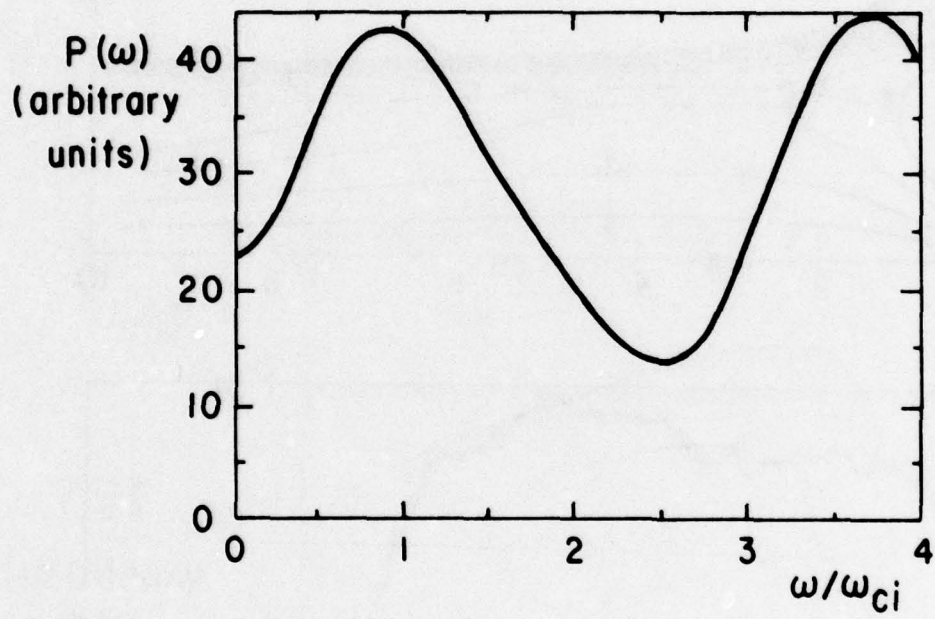


FIG. 4 A typical frequency spectrum for the case of Figs. 2 and 3.

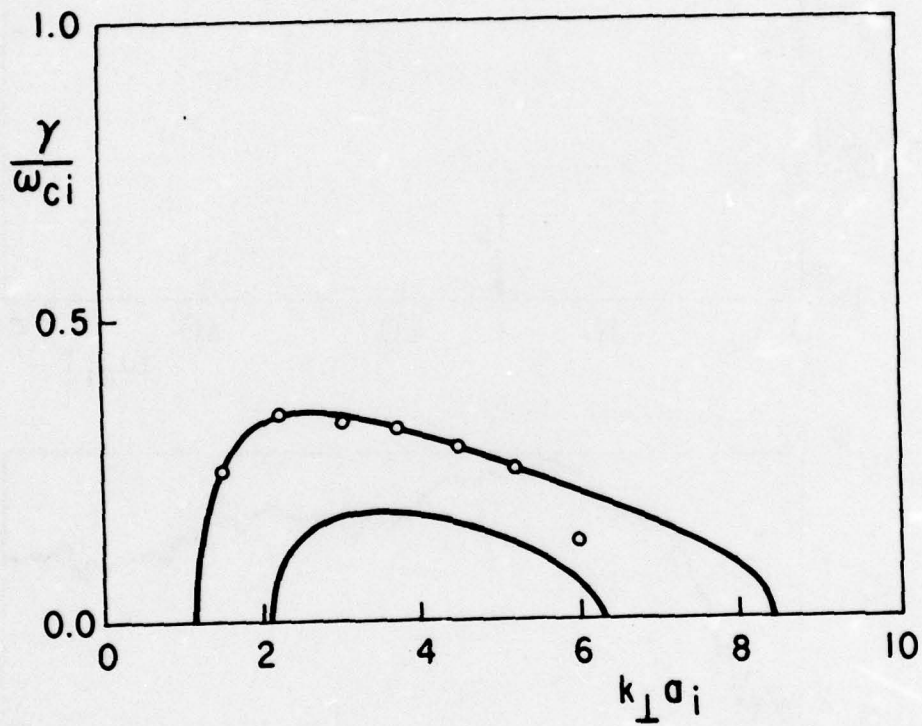


FIG. 5 Comparison of simulation growth rates (marked 0) with the linear nonlocal theory [3] (curves). Here,  $m_i/m_e = 100$ ,  $\kappa = 0.7$ ,  $\omega_{pe}^2/\omega_{ce}^2 = 0.15$ .

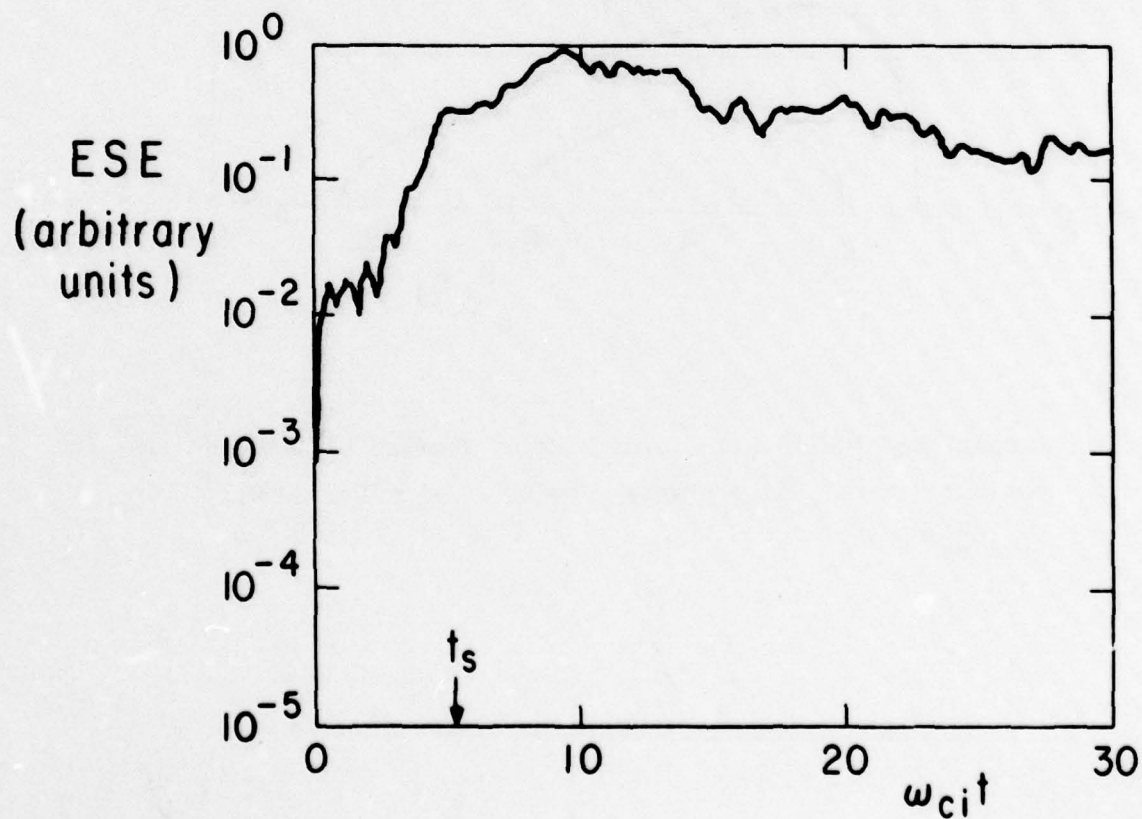
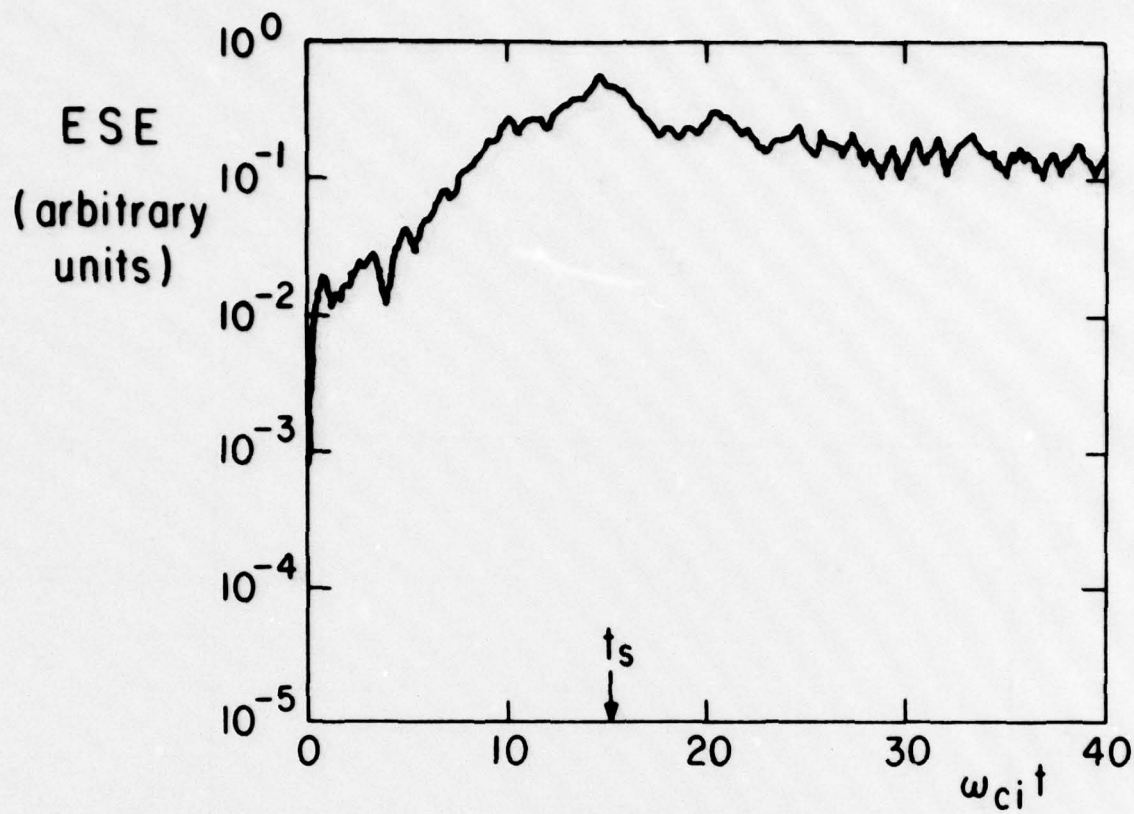


FIG. 6 Typical time evolutions of electrostatic energy (ESE) for (A)  $\kappa = 0.45$ , (B)  $\kappa = 1.0$ . Other parameters are  $m_i/m_e = 25$ ,  $\omega_{pe}/\omega_{ce} = 1$ .

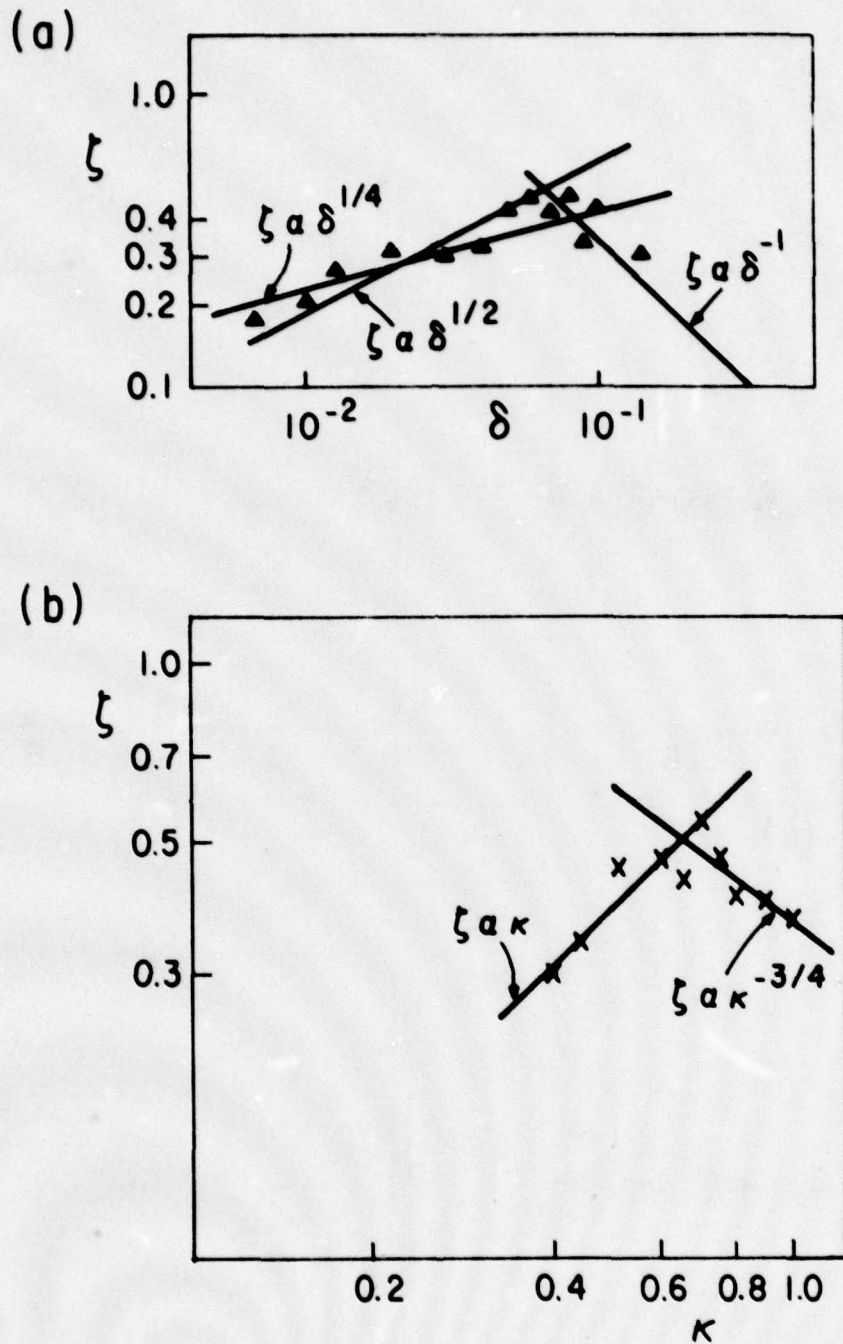


FIG. 7 Simulation saturation levels ( $\zeta \equiv e\phi/T_i$  at saturation) marked  $\Delta$  and  $\times$ . The lines are drawn to indicate the predicted slopes of nonlinear theories [2,9,12].  $\delta \equiv [(m_e/m_i) + (\omega_{ci}/\omega_{pi})^2]^{-1/2}$

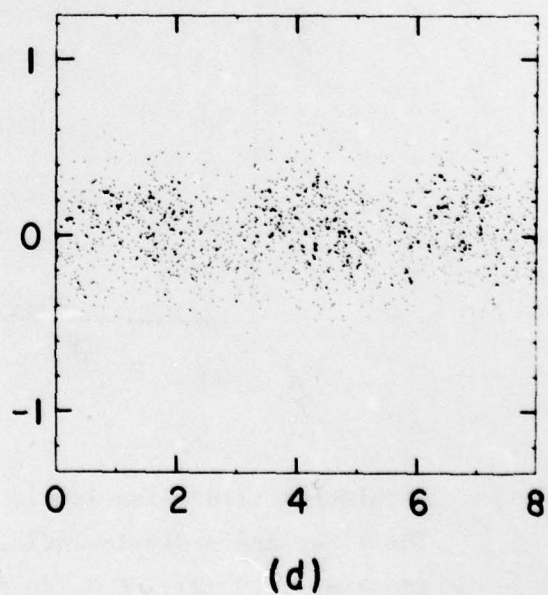
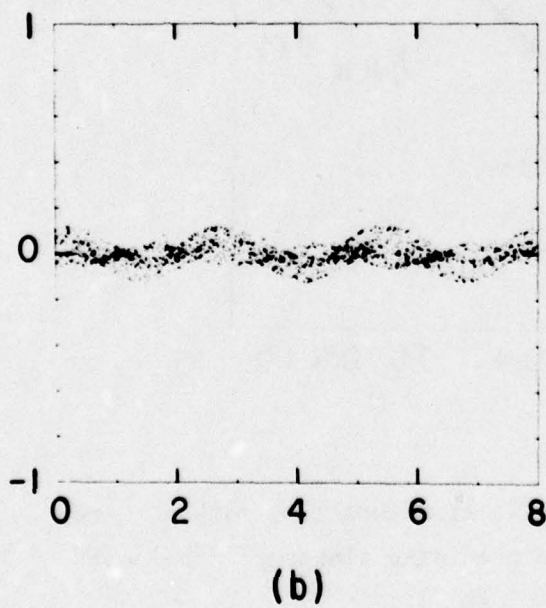
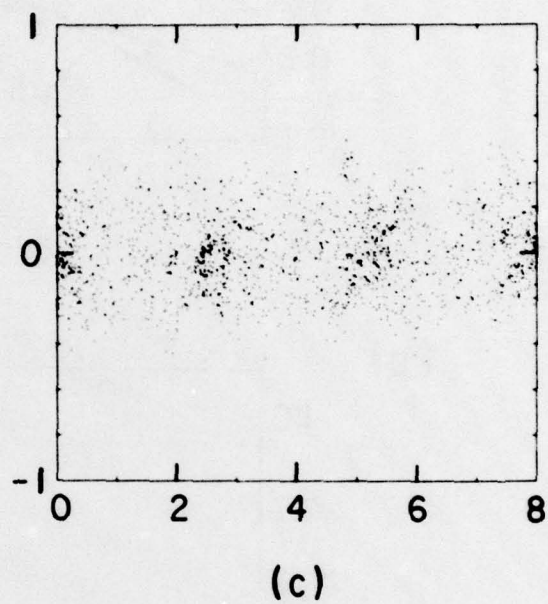
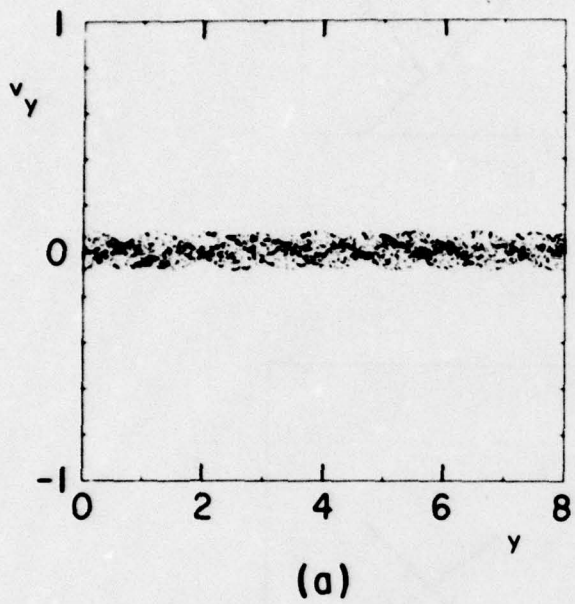
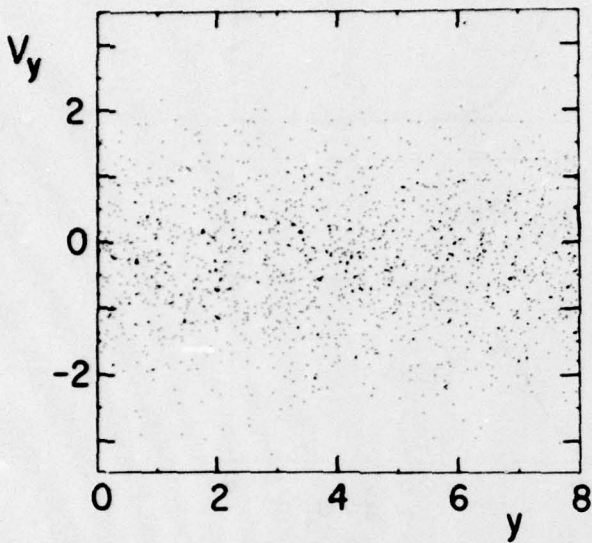
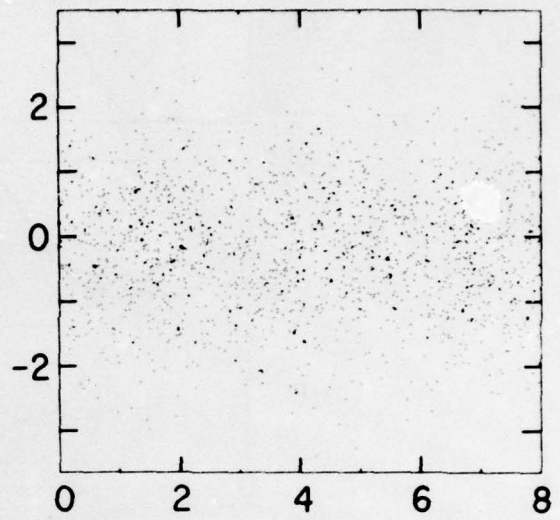


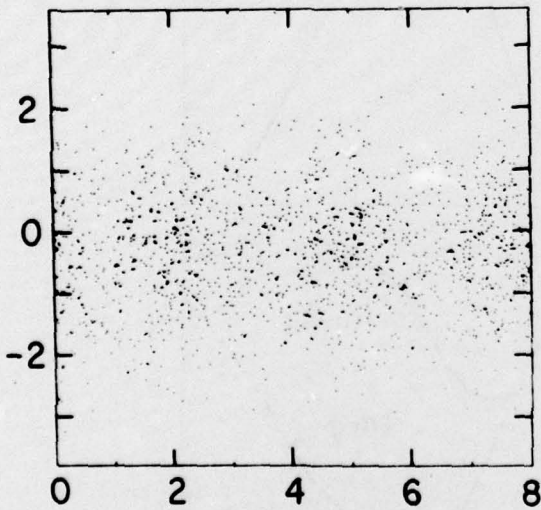
FIG. 8A Typical phase space pictures of electrons, at increasing times  $x$ .



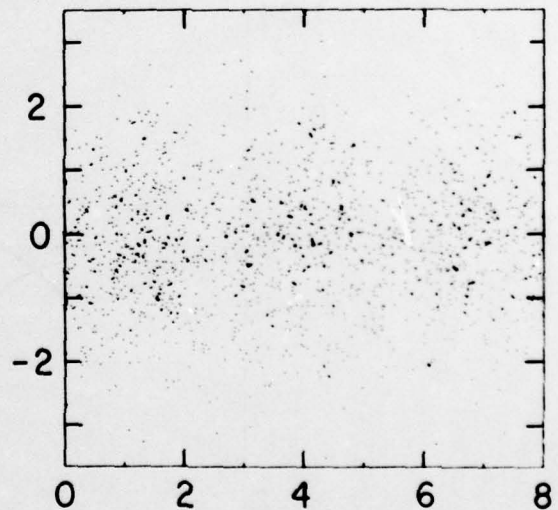
(a)



(c)



(b)



(d)

FIG. 8B Typical phase space pictures of ions.

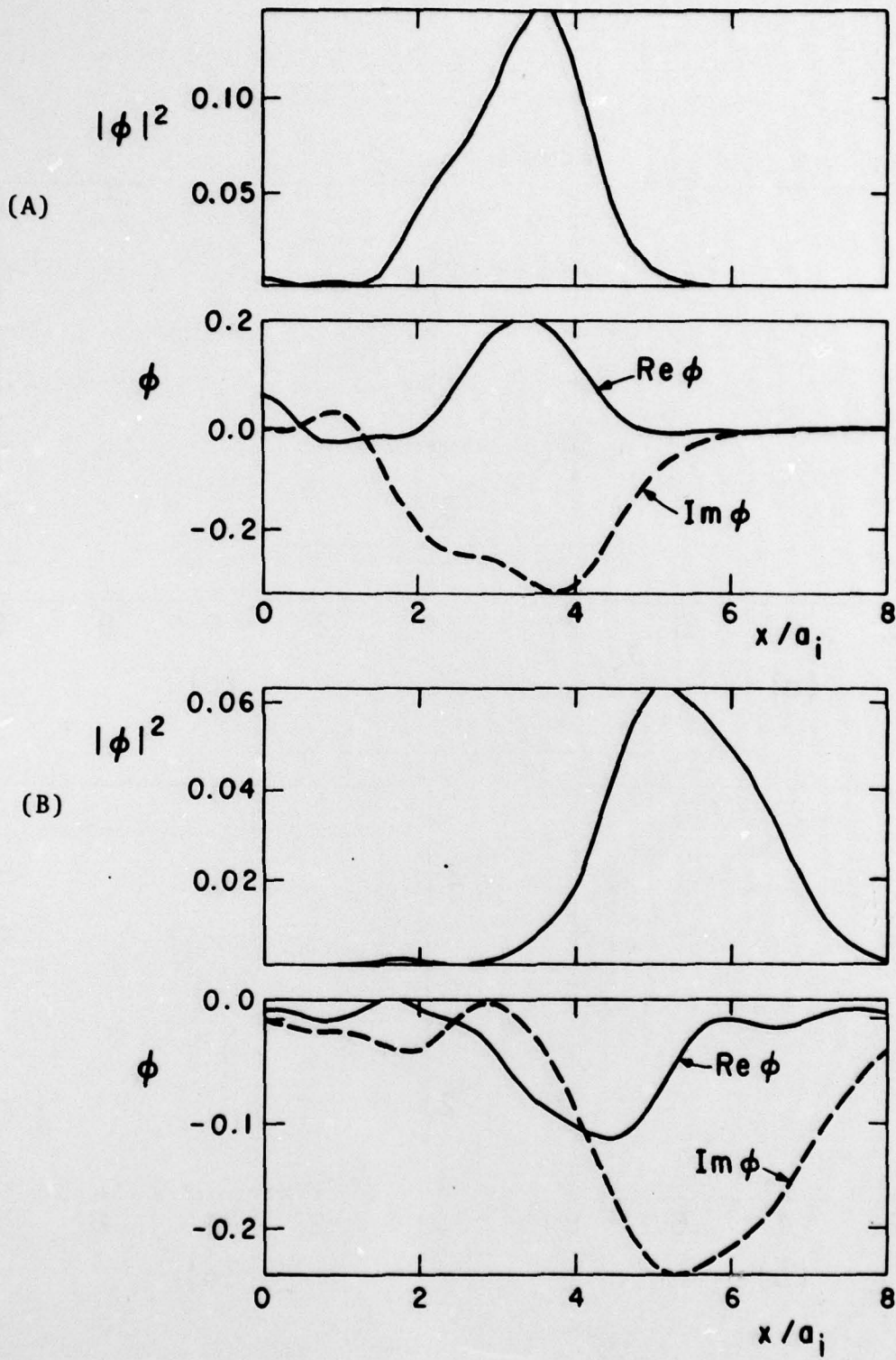


FIG. 9 Radial structure of potential for (A)  $\kappa = 1.0$  and for (B)  $\kappa = 0.5$ .

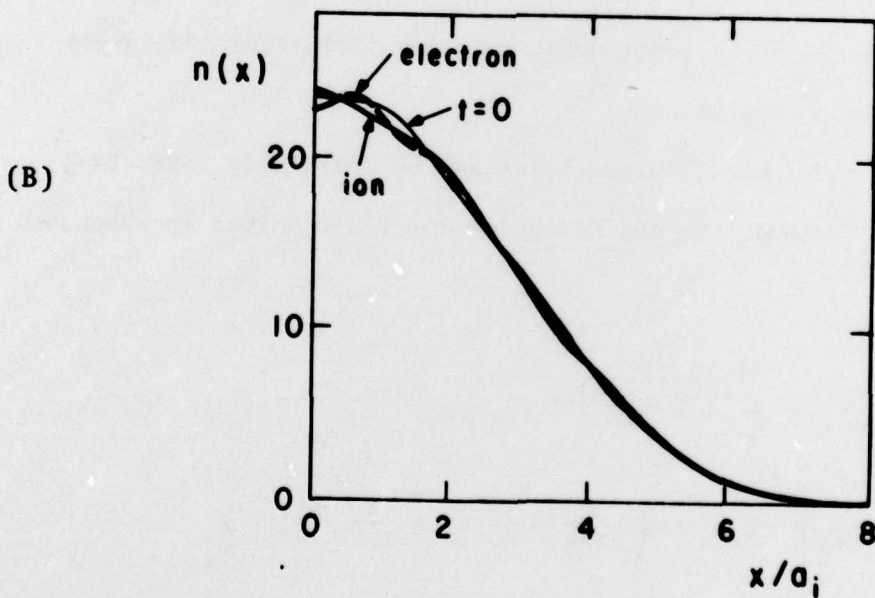
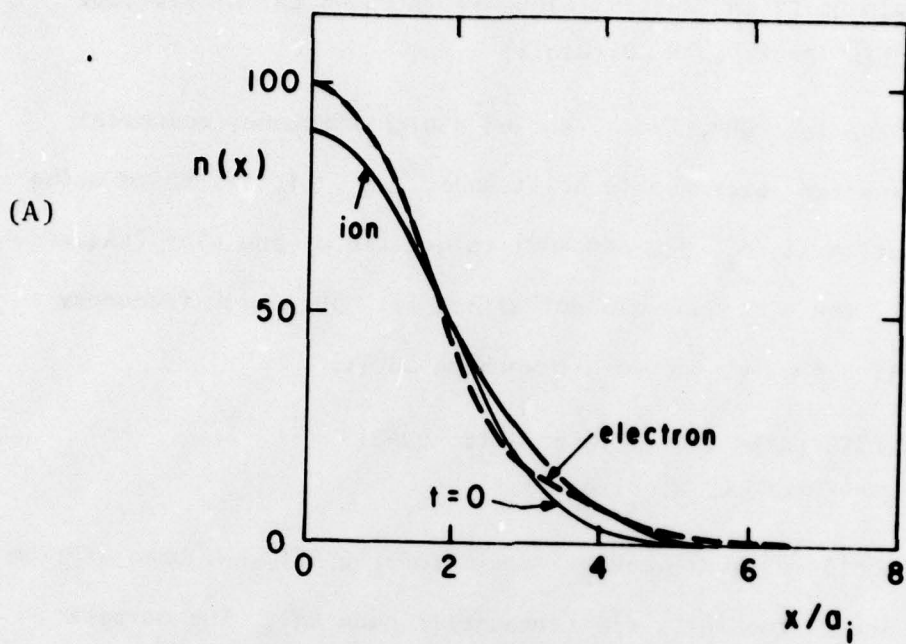


FIG. 10 The average radial density of (A)  $\kappa = 1.0$ ,  $\omega_{pe}^2/\omega_{ce}^2 = 1$ , and (B)  $\kappa = 0.5$ ,  $\omega_{pe}^2/\omega_{ce}^2 = 0.4$  for  $m_i/m_e = 25$ .

B. LOWER-HYBRID DRIFT INSTABILITY SIMULATIONS USING ESI HYBRID CODE  
 Yu-Jiuan Chen (Prof. C. K. Birdsall)

In the last QPR, Fig. 1 showed a high frequency component as well as the expected lower-hybrid drift mode,  $\omega/\omega_{pi} \sim 1$ . We tried using different mass ratios ( $m_i/m_e = 900$  and  $400$ ) to get rid of the high frequency response, however, these changes did not affect it. This high frequency component is still a puzzle, but we are working on it.

C. FIELD REVERSED LAYER SIMULATIONS IN 1d, QUAD1  
 D. S. Harned (Prof. C. K. Birdsall)

A nonlinear quasineutral Darwin Code, QUAD1, has been written using the framework of the fully electromagnetic code EM1. The purpose of this code is to provide insight into the problems of matching the plasma fields at the plasma-vacuum interface. This problem must be resolved before moving to a two-dimensional model to study field-reversed layers surrounded by a vacuum region.

The model uses ion particles and an infinitely conducting electron fluid background. In one dimension the field solver is expressed as

$$B_{z,n+\frac{1}{2}} = -c \Delta t \left( \frac{\partial E_{y,n}}{\partial x} \right) + B_{z,n-\frac{1}{2}}$$

$$E_{x,n+1} = -E_{x,n} - \left( \frac{1}{2\pi ne} \frac{\partial B_z}{\partial x} B_z + \frac{2}{nec} J_y B_z \right)_{n+\frac{1}{2}}$$

$$E_{y,n+1} = -E_{y,n} + \left( \frac{2}{nec} J_x B_z \right)_{n+\frac{1}{2}}$$

This model is essentially the same as that suggested by other groups working with quasineutral models [1,2,3]. The imposition of quasi-neutrality appears to prevent the application of the model in regions of low density ( $n \rightarrow 0$ ). Therefore, artificial methods of matching to the vacuum field equations must be used at some point in the plasma where the Courant condition  $\frac{\Delta t}{\Delta x} < \frac{1}{v_A}$  breaks down.

At present the code exists in periodic and bounded (conducting wall boundaries) forms. It is in its preliminary testing stages. The initial version solved the field equations with a leap-frog method. However, to eliminate non-physical high frequency effects this has been changed to a predictor-corrector scheme.

#### REFERENCES

1. J. A. Byers, B. I. Cohen, W. C. Condit, J. D. Hanson, "Hybrid Simulations of Quasineutral Phenomena in Magnetized Plasma", *Journal of Computational Physics*, Vol. 27, 363-396 (1978).
2. A. Friedman, R. N. Sudan, J. Denavit, "A Linearized 3-D Hybrid Code for Stability Studies of Axisymmetric Field-Reversed Equilibria", Proceedings of the Eighth Conference on Numerical Simulation of Plasmas, Monterey, California, June 28-30, 1978.
3. D. W. Hewett and A. G. Sgro, "Zero Electron Mass Hybrid Simulation", Proceedings of the Eighth Conference on Numerical Simulation of Plasmas, Monterey, California, June 28-30, 1978.

#### D. CONTROL OF UNWANTED BEAMING INSTABILITIES

Yu-Jiuan Chen (Prof. C. K. Birdsall)

The quiet start loader in ES1 used to study the lower-hybrid drift instability has a physical multibeam instability which may affect the simulation results. As the same problem occurs in other simulations some effort has been made to study the multibeam instability. Results in Gitomer and Adams [1] have been reproduced exactly. Due to the analogy between the multibeam and two-stream instabilities, we tried to stabilize the multibeam instability by adding a small thermal spread  $VT1$  to each beam. As shown in Fig. 1 (A, B and C), associated with a larger thermal spread is both a higher initial electric field energy, and a shorter period linear growth before the field energy reaches saturation. It is noticed that all the saturation levels are the same as that in the randomly Maxwellian case. A reason that a warm multibeaming plasma system will reach the thermal equilibrium faster is that each beam already is randomly Maxwellian. The parameters we used are as follows: time step  $DT = .04\tau_p$ , cell size  $x = \lambda_D$ , total plasma length  $L = 128\lambda_D$ , number of large groups  $NLG = 128$ , number of particles  $n = 16384$ , and the thermal spread added to each beam  $VT1 = 0.0, 1 DV, \text{ and } 0.5 DV$ , respectively.  $\tau_p$  is the plasma oscillation period. The DV in ES1 code is defined as  $DV = 5. * VT2 / ( N - 1 )$ .

#### REFERENCE

- [1] S. J. Gitomer and J. C. Adam, "Multibeam Instability in a Maxwellian Simulation Plasma", Phys. of Fluids, Vol. 19, No. 5, P. 719 (1976).

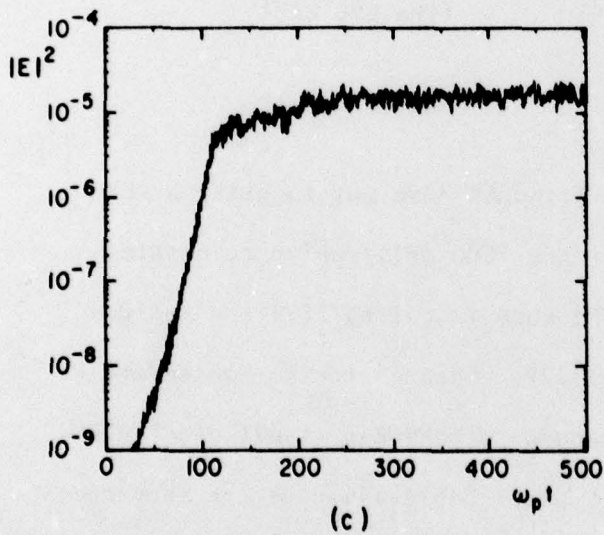
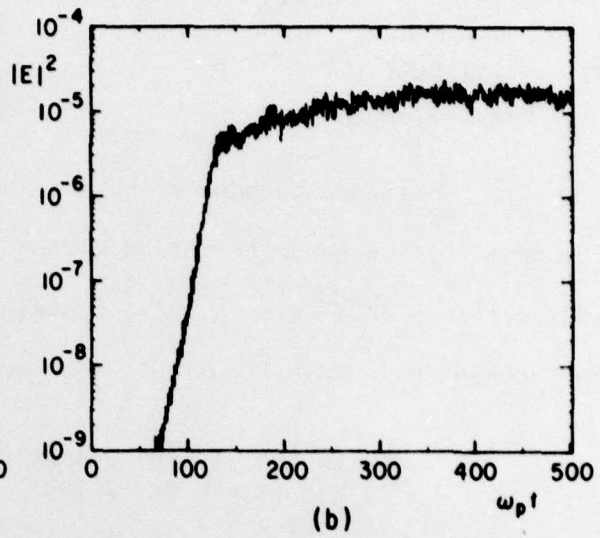
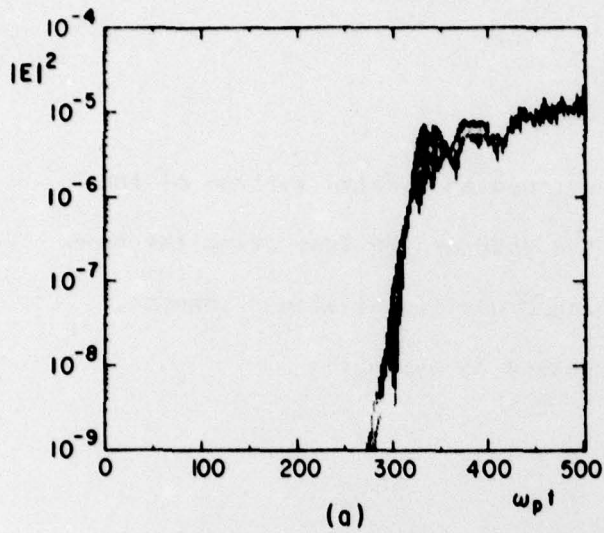


FIG. 1 Electric field energy versus time for the multibeam instability simulation. The beam's thermal spread  $VT_1$  is 0., .1 DV and .5 DV, respectively, in (A), (B) and (C).

*Section III*  
CODE DEVELOPMENT and MAINTENANCE

A. ES1 CODE

A. Friedman

Bruce Langdon of LLL has developed an updated version of the ES1 code which can now be run on either the 7600 or the Cray using the same source file. This version, also containing other miscellaneous changes, is documented in ES1REP, which can be accessed by typing:

```
FILEM RDS 339650 .ES1 ES1LIB / T V
ES1LIB ES1REP DR. / T V
TRIX AC / T V
PRINT(<USC CCC ES1REP BOX BNN>) [trix print doesn't yet
                                  like USC UCB]
END
```

See also the LIBRIS writeup for ES1.

Stephen Au-Yeung and Alex Friedman have put together a version of the ZED-compatible code ESZ (for the 7600 only) which reinstates the "original" history plots of ES1. The code is called ESZ1 and resides in Filem directory SAY76 of user number 1222. Changes to the source are flagged by "CA" in the first column (changes to make ESZ itself use "CADD"). Variables associated with the "original" plots typically have the same names as in the original ES1 with "OL" appended. The input variable "IFOL" can be set to zero to suppress these plots if they are not wanted.

B. EM1 CODE

No special report.

C. EZOHAR CODE

No special report.

D. ESI + EFL CODE

No special report.

E. RINGHYBRID CODE

Alex Friedman

This code is under active development and testing on ion ring and layer problems. We have had some success in creating equilibria corresponding to high-beta mirror plasmas, with plasma radius two or three times the nominal gyroradius, but these equilibria exhibit large fluctuations and are thus too "noisy" for use. More flexibility has been built into the particle injector, and with experience we expect to be able to generate reasonably quiet equilibria. We have decided to apply the code initially in its present form to field-reversed mirror configurations, in order to gain experience before attempting to modify the algorithm in the manner described in the previous QPR. The modifications will eventually facilitate the making of runs not incorporating the cold fluid ion component now assumed to be present.

F. RJET DEVELOPMENT

A. Friedman

The UCB RJET is up and running, complete with the Versatec printer as an independently controlled output device. Our initial impressions are very favorable, with turnaround time and output quality good. We are grateful to Harry Massaro and everyone else who helped get the system working.

Some notes on usage follow.

To send listings, print files, etc. to the Versatec printer:  
NETOUT [UCB] PRINTFILELIST [OPTIONS] BOX BNN ID / T V

Options: B. 8-bit Ascii file  
L. file contains lines longer than 120 characters  
S. add sequence numbers (6-bit Ascii files only)  
ULC. 6-bit upper/lower case file  
(there are other options as well)

"UCB" is optional if one is logged onto a user number with UCB as the default destination. Instead of NETOUT one can use BANNER, which has a wider range of options, including "ccsp." and "seq." from ALLOUT.

To send plot files to the Versatec printer:

NETPLOT [UCB] PLOTFILELIST [OPTIONS] BOX BNN ID / T V

Options: F. necessary for FR80 format plot files.  
L. for "high-resolution" (10"x10") plots -  
default is 5"x5". The larger plots do  
not fit entirely on one 8.5"x11" page.  
(there are other options as well)

To query the progress of files through the network:

(CTRL-E)RP? UCB and/or YLUS UCB / T V

To send selected frames of a plot file to the Versatec while viewing the frames on the Tektronix terminal, using utility routine TEK/PLOT (for DD80 files) or FR80/PLOT (for FR80 files), type "USC", and when the routine asks for the destination reply "UCB".

To extract selected frames of a DD80 plot file without having to view the file (and wait for TEK/PLOT to draw the frames), use the utility routine DDEX, described elsewhere in this report. It is helpful to have your program generate a frame index to facilitate use of this utility. Large plot files can be sent to microfiche, and selected frames sent to the Versatec; this will avoid tying up the printer for excessive periods of time if your plot file consists of hundreds of frames.

Control of the printer:

Using the operator's console (the teletype by the pdp-11), one has some control over the printer and the print queue. When a file begins to list, the teletype will print its name, the word "begin", and a sequence number.

To kill a printout: PRNT KILL \*\*\*, where \*\*\* is the sequence number  
(leading zeros can be omitted)

To re-queue it: PRNT REQU \*\*\*

To take the printer  
offline, in order  
to add paper, etc.: PRNT DOWN

To bring the printer  
back online: PRNT UP

G. DDEX Utility Routine  
Steve Au-Yeung and Alex Friedman

dd80 Frame Extraction Routine

Availability: NMFEC a-machine  
filem rds 1222 .say76 ddex

ddex allows the user to extract selected frames from one or more dd80 graphics files and write them to a smaller dd80 output file which can be processed in a wide variety of ways. The intended purpose was to facilitate use of the "high-quality hardcopy" option of the utility routine FROG. Since this form of output is costly, large amounts of graphical output should not normally be processed in this manner. In addition, the shorter output files (1) may be used to create 35 mm negatives suitable for white-on-black projection via give to user - 1 ( $\frac{1}{2}$  frame) or FROG (full frame), (2) may be sent to the user's usc versatec printer via netplot, or (c) may be sent to the nips processor via nipit.

If your program generates fr80 files to obtain a dd80 file use the utility routine fr80edit. This is especially useful if your code runs on the Cray which supports only fr80 files. Send the fr80 files to the 7600 via "netout a filenames b."

Usage: the main usage form is exemplified by:

```
user:          ddex / t v
routine/user:  infile: dxmyplots1
routine/user:  box and id: box bnn plots1_ex
routine/user:  > 4 17 35 20
routine/user:  > end
routine:       all done
```

The id string consists of up to 18 alphanumeric characters. Embedded spaces may appear incorrectly and are not recommended. Use "  " instead. Note that the frames need not be in order as they are ordered

before extraction. The output file name is constructed from the id line; it is of the form dx [first eight characters of id]. If id consists of fewer than eight characters, the filename is right-filled with asterisks to ensure a ten-character file name. If the file to be created already exists, the user is given the options of overwriting it or entering a new id line. Some shorter usage forms are allowed; in particular, the input file name may be entered on the execute line, or after the command "infile".

ddex is actually a "lib" file; the sources and binaries are contained within the file itself, as is this documentation.

Options (all may be abbreviated by first letter):

thru	extract all frames between preceding and following entries, inclusive.
infile	change the input file. All selected frames of the previously opened file are extracted before opening the new file.
end	terminate, processing all selected frames.
quit	like end, but when entered after infile command causes previously entered frames to be extracted without changing the input file or causing termination; more frame numbers can then be entered. (useful when an "i" has inadvertently been entered).
nochar	eliminates all alphanumeric characters from all frames. Useful for suppressing crowded labels on axes when preparing figures for publication.
offset	set offset for calculation of frame numbers. Useful, for example, if the user is referring to a previously generated "nipit" output to determine frame numbers; tekplot considers frame 0 to be blank, and frames 1 and 2 to contain header information, so that for tekplot (and ddex) plot information normally begins in frame 3. On the nips output, frame 1 contains plot information, so the user may enter "offset 2" and then the nips frame numbers.

Restrictions: at present ddex does not accept file families.

If a frame overlaps the end of one file and the beginning of the next, the routine will fail.

Support: this routine was developed, and is supported, by Stephen Au-Yeung and Alex Friedman at the University of California, Berkeley. Inquiries / gripes should be directed to either of the above at (415) 642-1297 or 642-3477.

*Section IV*  
PLASMA SIMULATION TEXT

No special report.

*Section V*  
SUMMARY OF REPORTS, TALKS AND PUBLICATIONS  
IN THE PAST QUARTER

No special report.

*Errata*

In the QPR for the previous quarter:

page 8      the footnote's author should be Davidson  
page 16     Section B, Line 2: to read ..."  $x$  and  $k_y$  "...

DISTRIBUTION LIST

Contractor (DOE)

Robert Price  
Donald Priester  
Walter Sadowsky  
Oscar Manley

Contractor (ONR)

Padgett (plus 67  
to ONR list), Keith,  
Grisham, Siambis

Northwestern Univ.

Denavit

- 36 -

Naval Research Lab

Boris, Winsor, Lee

Berkeley Campus

Birdsall, Cuen, Harned, Buchanan,  
Lee, Lichtenberg, Lieberman, Arons,  
McKee, Chorin, Au-Yeung, Friedman

SAI

Klein, McBride, Wagner

IBM Palo Alto

Gazdag

Berkeley Lab (LBL)

Kunkel, Kaufman, Cooper, Maria Feder  
(library), Pyle

EPRI

Gough, Scott

Livermore (LLL)

Byers, McNamara, Maron, Kruer, Langdon,  
Lasinski, Max, Fuss, Bruijnes, Tull  
Killeen, Marx, Mirin, Fries, Harte,  
Cohen, Taylor, CTR Library, Berk  
Briggs, Lee, Chambers, Smith, Matsuda

General Atomic

Helton, Tommey (Library)

Israel

Gell, Cuperman

Univ. of Reading

Hockney

Inst. fur Plasmaphysik

Biskamp

U.C. Davis

DeGroot

Univ. of Maryland

Gullory, Sternlieb

Bell Labs

Hasegawa

U.C.L.A.

Dawson, Lin

Univ. of PA

Fawley

Culham Lab

Roberts, Eastwood

Stanford

Buneman, Barnes

Plasma Physics Inst. Nagoya

Kamimura

Columbia Univ.

Chu

MIT

Bers, Berman

Princeton PPL

Chen, Okuda, Graydon (Library), Nevins,  
Tang

NYU

Univ. of Wisconsin

Grad Shohet

Oak Ridge NL

Meier, Dory, Mook (Library)

Univ. of Texas

Macmahon, Horton

Los Alamos SL

Lindman, Nielson, Burnett (Library)  
Gitomer, Lewis, Hewett, Forslund,  
Godfrey

Univ. of Iowa

Knorr, Joyce, Nicholson

Stevens Inst.

Rosen

Berkeley Space Sciences

Lab

Hudson, Potter

Cornell Univ.

Gerver

ITT-Spain

Canosa

Univ. Rochester

Albritton

U.C.-Irvine

Rynn

Sandia Laboratories

Freeman, Poukey

NASA

Hohl

Bhabha Atomic Research Centre

R.N. Aiyer

Kirtland AFB

Pettus

Mission Research Corp

W. E. Hobbs

C. E. Rathmann

NOTE: Please send advice on additions/deletions to Prof. C.K. Birdsall. If you want your copy or an additional copy to be sent to your library, please send complete address.